Journal of Advanced Research in Fluid Mechanics and Thermal Sciences

Journal homepage:
https://semarakilmu.com.my/journals/index.php/fluid_mechanics_thermal_sciences/index
ISSN: 2289-7879

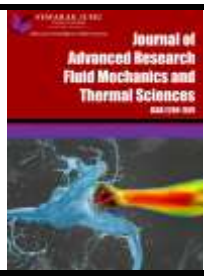

Heat Transfer Improvement by Exploitation of Nanofluids in a Tubular Heat Exchanger

Salim Bennoud[1,*], Merouane Salhi[2]

[1] Institute of Aeronautics and Space Studies, University of Blida 1, Algeria
[2] Energetic Process and Nanotechnologies Laboratory LPEN, Mechanical Engineering Department, Faculty of Technology, University of Blida 1, Algeria

ARTICLE INFO

Article history:
Received 5 March 2024
Received in revised form 29 July 2024
Accepted 13 August 2024
Available online 30 August 2024

Keywords:
Heat exchanger; nanofluid; heat transfer; tube banks; numerical analysis; Nusselt number

ABSTRACT

The enhancement of heat exchanger performance without an increase in its surface area constitutes a real challenge. It is vital to consider this challenge to improve processes and increase the efficiency of energetic and thermal systems. Nanofluids have recently been used in many industries and engineering applications, especially in heat exchangers. The increase in the application of nanofluids is due to their numerous attractive properties, such as the capacity to improve heat transfer and thermal conductivity. Most contemporary problems of nanofluid heat exchangers, such as determining nanofluid characteristics and their exploitation in CFD software, have been the subject of recent scientific papers. This work focuses on clarifying all the steps that must be taken to carry out any correct study concerning nanofluid heat exchangers. The properties of nanofluids are calculated using adapted models and formulas. This modeling uses mathematical expressions permitted to cover a large range of applications. The evolution depends on the chosen nanofluid, the variation of the temperature and the concentration rate of the nanofluid. Polynomial interpolations for these properties are obtained and injected into CFD software (FLUENT code) to carry out simulations using various nanoparticles. This paper conducts a numerical analysis of a microtubular heat exchanger to investigate its thermal impact, particularly on the Nusselt number and the coefficient of heat transfer convection. The application was developed for six different nanoparticles (Al, Al_2O_3, Cu, CuO, TiO_2, and SiO_2) with a concentration of nanofluids ranging from 0.5% to 5%. The obtained results present the behavior of nanofluids and the heat transfer improvement. The Nusselt numbers of SiO_2 and TiO_2 are greater than the other nanofluids (Al_2O_3, Al, Cu, CuO). They can reach up to 64% and 61% for SiO_2 and TiO_2 respectively, compared to water. For a fixed temperature, the effect of the concentration on conductivity, density, and dynamic viscosity is proportional for all considered nanofluids. On the other hand, the Prandtl number, specific heat, and volume expansion decrease with an increase in concentration. The improvement of the exit temperature at m=0.05kg/s can reach up to 12.2% and 2.1% for Al and Cu respectively, compared to water.

* *Corresponding author.*
E-mail address: bensalimen2006@yahoo.fr

https://doi.org/10.37934/arfmts.120.2.137154

1. Introduction

Today's technological advances allow more precise temperature control and improve energetic performance for domestic, commercial, and industrial needs. These advances require the use of a device capable of extracting heat from the medium to be cooled in order to reject it to an external medium. This device necessarily obeys the principle of heat transfer [1].

Heat transfer is a field of main importance in the domains of industry and technology. It manifests in various forms, such as radiation, conduction, and convection [2]. The process of convection is most targeted in certain very specific areas, such as the cooling of processors and electronic components, radiators, heat exchangers, etc. The intensity of heat transfer mainly depends on the conductivity and heat capacity of the applied fluids [3].

So, improving processes and increasing the efficiency of energetic and thermal systems, especially heat exchangers, constitute a veritable technological challenge. Moreover, multiple problems can appear in conventional heat exchangers. These problems are due to the increase in the quantity of metallic material leading to the tubes fouling and the degradation in heat transfer and pressure performances. For these reasons, it is essential to have new advances and solutions for these problems. The enhancement of the heat exchanger performance without an increase in its surface area can be presented as an appropriate and suitable solution. Various approaches based on the proposal of the introduction of changes to fluid properties have recently been developed (the introduction of nanoparticles for example). These approaches can be achieved using various models and correlations that can predict a wide range of experimental and theoretical data. This variety firstly requires the comprehension of different relative mathematical relations and models, and lastly the assemblage of these models in a numerical scheme. However, the determination of characteristics of nanofluid heat exchangers and their exploitation in CFD software have become an interesting subject of recent research works. Any developed software associated with these problems must focus on correlations concerning the determination of thermophysical properties as an important priority and obligation.

In the past few decades, a new type of fluid, known as nanofluid, has emerged. Nanofluid is a base fluid, such as water, glycol water, and mineral oil, to which metal nanoparticles (Al, Cu, Ag, Au, etc.) or metallic or non-metallic oxides (SiO_2, Al_2O_3, TiO_2), and other entities (allotropic forms of carbon) are added and dispersed [4-7]. The nanoparticles are nanometer-sized substances.

It is approved that nanofluids can increase the heat transfer compared to conventional fluids. This improvement is realized by changing the thermal conductivity of the base fluid. This advantage makes nanofluids a promising new technology in the context of heat transfer [6-8].

Sonawane *et al.,* [9], Shahrul *et al.,* [10], and Chandrasekar *et al.,* [11] studied the investigations on thermophysical properties. They discussed the performance evaluation of nanofluids using theoretical and experimental methods.

Many studies have shown examples of the wide range of applications of nanofluids in different disciplines, such as technologies and industries. Nanofluids are usually employed in product quality enhancement, engine cooling, nuclear systems cooling, thermal energy improvement, and air conditioning and refrigeration systems. This extension of applications is mainly due to the thermal potential acquired by the base fluid through the introduction of nanoparticles [9,12-15].

However, among all possible applications of nanofluids, particular attention is given to the field of nanofluid application in the technology of heat exchangers. This important attraction allows the use of nanofluid heat exchangers to become very important. The exploitation of nanofluid heat exchangers avoids high maintenance costs as well as service loss and ensures that the devices work at high levels of pressure and temperature.

Improving the performance of these heat exchangers is therefore a priority that can be achieved by several methods (namely, passive methods and active methods or others). These methods permit the improvement of heat transfer processes by increasing the exchange rate. An improvement in exchange rate can be obtained by increasing the velocity of heat transfer. This method tries to change the fluid nature by the introduction of nanoparticles [16].

Several papers, both experimentally and theoretically, investigated the evolution of various types of nanofluid heat transfer exchangers. Pandya *et al.,* [17], and Sarafraz and Hormozi [18] studied the use of nanoparticles in fluids in plate heat exchangers. They worked on the performance of various types of metal oxide nanoparticles dispersed in water and other base liquids. However, Shahrul *et al.,* [19] experimentally studied the heat transfer coefficient of forced convection and the characteristics of Al_2O_3-gamma nanofluid in a horizontal shell-and-tube heat exchanger. Another example presented by Wang *et al.,* [20] discussed the heat transfer characteristics of tube banks heat exchangers and compared them with those of shell-and-tube heat exchangers.

A review of the previous literature and references confirms that the considered nanofluids have new properties, which are different from those of base fluids. The most significant thermophysical properties affected by the change in the base fluid nature are thermal conductivity, viscosity, specific heat, and density.

The variation of novel thermophysical properties of the nanofluids can be determined by correlations. The correlation of the thermal conductivity using Kim and Chon model was calculated by Chon *et al.,* [21]. Moreover, the thermal conductivity can be obtained using different correlations in review papers by several authors [22-26].

Results presented by different authors measured the dynamic viscosity of nanofluids [27-29]. They showed that this property does not depend only on the volumetric concentration of nanoparticles in the base fluid. They also mentioned that other parameters, such as the shape and size of the particle, the combinations of the mixture, and the used surfactants, can affect this property measurement.

However, Shin and Banerjee [30] calculated the specific heat of nanofluids, which is also considered as an important thermophysical property, and explained its performance evolution.

The research described in this work aims to distinguish and analyze the problem concerning the analysis of the characteristics of fluid flow and heat transfer. The considered problem is focused on tube banks heat exchanger. This work will numerically investigate some effects of various nanofluid properties to improve CFD calculations on heat exchangers. The principal objective is to increase the capacity of heat transfer and find the best combination of Nanofluids–Concentration. The mathematical treatment permits the selection and development of polynomial correlations of all nanofluid characteristics. The polynomial interpolations are obtained and injected into CFD software (FLUENT) to carry out simulations. They are calculated using adapted models according to the variation of the temperature and various nanoparticles (Al, Al_2O_3, Cu, CuO, TiO_2, and SiO_2).

2. Materials and Methods

2.1 Tube Banks Heat Transfer

Actually, many types of heat exchangers can be found, plate, shell-and-tube, tube banks, etc [17-20]. The tube banks heat exchangers are the most required type for different thermal systems.

As a basic idea, the fluid is perpendicularly flowing to the axis of the cylinder. U_{inf} and T_{inf} are respectively the fluid velocity and temperature at infinity upstream. Figure 1 shows that a wake forms downstream of the flow. This wake leads to an inhomogeneous distribution of the variable coefficient

on the periphery of the cylinder. It is to be noted that an average convection coefficient for the entire periphery at temperature T_s must be defined.

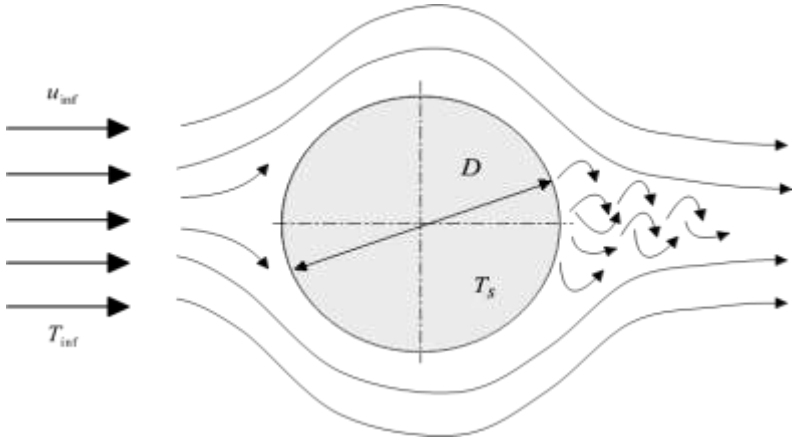

Fig. 1. Flow around a cylinder

However, many industrial installations consist of rows of parallel tubes immersed in a perpendicular flow to their axis. The tubes can be aligned or staggered, as shown in Figure 2.

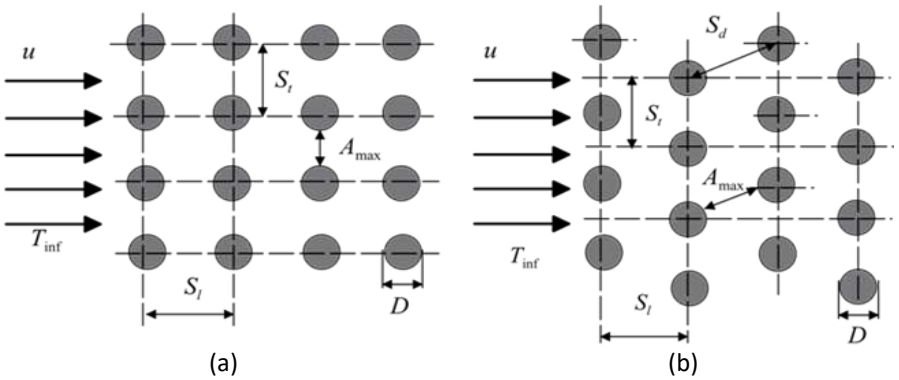

(a) (b)

Fig. 2. Flow around a tube banks: (a) aligned arrangement; (b) staggered arrangement

In several heat exchanger configurations, the tubes are arranged as a bundle or a bank in an in-line or staggered manner. In the case of tube banks exchangers, the first fluid flows over the tube banks while the second fluid with a different temperature passes through the tubes (see Figure 3).

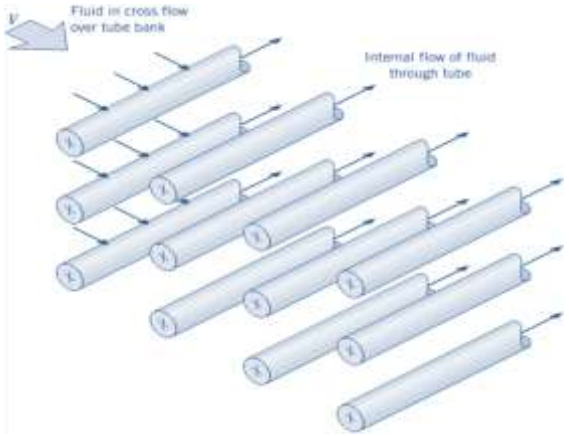

Fig. 3. Tube banks in cross flow [3]

The heat transfer characteristics of tube banks are governed by several equations and models with the aim to obtain polynomial correlations. These correlations permit the control of the characteristic's behavior of the considered problems.

The numerical simulation of free convection, forced convection, and mixed convection of the nanofluid is controlled by the continuity, momentum, and energy equations [3,4,31]. These equations, known as the Navier-Stokes equations, are complex and need to be simplified using assumptions and specific conditions. The computational fluid is Newtonian, incompressible, and steady state. The thermophysical properties of the fluid are constant and its inlet velocity is uniform.

In this study, the Reynolds Average Navier-Stokes model in its dimensionless form is chosen to solve the heat transfer and fluid characteristics [3,4,31].

Once the governing equations are numerically solved using FLUENT code, the analysis of the thermal and fluid dynamic must be provided.

The heat transfer rate by diffusion based on Fourier's law can take various forms. The differential form of the conduction, in the case of one-dimensional flux, is given by

$$\vec{Q} = -K\,S\,\frac{dT}{dx}\vec{i} \tag{1}$$

where K is the constant coefficient of thermal conductivity, S is the total surface area, and dT/dx is the temperature gradient.

The heat transfer rate for thermal convection is given by

$$\dot{Q} = h\,S\,\Delta T \tag{2}$$

where h and ΔT are the overall heat transfer coefficient and the mean temperature difference between the tube wall and the bulk of the fluid, respectively.

Eq. (1) and Eq. (2) present the basis of design calculations for all types of heat exchangers.

Several empirical correlations for approximating convective heat transfer coefficients were developed and investigated, experimentally and theoretically. Dimensionless numbers such as Nusselt number, Reynolds number, and Prandtl number are employed to express them.

The Nusselt number is defined as the dimensionless relation among conductive heat transfer and convective heat transfer of the studied fluid. It is described by substituting the heat transfer coefficient (h) and thermal conductivity coefficient (K) from Eq. (1) and Eq. (2), as follows

$$Nu = \frac{h\,D}{K} \tag{3}$$

where D is a characteristic length.

The case of forced convection is encountered very often in practice in heat exchangers of all kinds. The Reynolds number is the essential parameter that characterizes the flow regime. This number can be written as

$$R_e = \frac{\rho\,V\,D}{\mu} \tag{4}$$

where V is the velocity in the cross section, D is the characteristic diameter of the tube, and ρ and μ are the fluid density and viscosity respectively.

Figure 1 above shows that the heat transfer flow around cylinders is characterized by boundary layer development and separation. The flow is strongly influenced by the nature of these characteristics at the surface.

However, many correlations that include those of the tube banks heat exchanger are available in previous studies [21-27]. These correlations can be applied to clarify the enhancement of thermal characteristics for all similar configurations. All presented correlations take the Nusselt number as a central parameter in their heat transfer analysis. For liquids, the correlation concerning the Nusselt number is treated as a function of Re and frequently correlated according to the Hilpert correlation. This correlation can be generalized to also apply to cross flow around other noncircular shapes [3,25,27,31]. The empirical correlation due to Hilpert is given as

$$\overline{\mathrm{Nu_D}} = \mathrm{C}\ \mathrm{Re_D^m}\ \mathrm{Pr}^{0.33} \tag{5}$$

where Pr is the Prandtl number, and C and m are given by the experimental data according to Re number values. These experimental data can be found in previous works and references [3,31].

This correlation is very useful for a number greater than 10 rows of tubes in a staggered arrangement, Pr>= 0.7 and 2000<Re<40000.

The staggered arrangement leads to stronger turbulence and therefore a higher exchange coefficient than for an aligned tube. The correlation in Eq. (5) can extend to all fluids through the insertion of factor 1.13 and becomes as follows [3,31]

$$\overline{\mathrm{Nu_D}} = \frac{\mathrm{hD}}{\mathrm{K}} = 1.13\ \mathrm{C_1}\ \mathrm{Re_D^m}\ \mathrm{Pr}^{0.33} \tag{6}$$

For fewer rows, tubes number <10, a correction factor (C_2) may be applied such that [3,31]

$$\overline{\mathrm{Nu_D}} = \frac{\mathrm{hD}}{\mathrm{K}} = 1.13\ \mathrm{C_1}\ \mathrm{C_2}\ \mathrm{Re_D^m}\ \mathrm{Pr}^{0.33} \tag{7}$$

The values of the constants in our study are: C_1=0.452, C_2=0.97, N=7 and m=0.568 for the staggered configuration.

The Reynolds number is designed in these configurations by the maximum flow velocity. This maximum flow velocity is observed for the planes designated by Amax for both cases (Amax is the smallest cross-sectional flow area between tubes in the bank). It is calculated using the spacing between the tubes (ST), the fluid arrival velocity (V) and the diameter of the tubes (D). It is given by Vmax=(V.ST)/(ST-D) for an aligned arrangement, and Vmax=(V.ST)/2(ST-D) for a staggered arrangement. The tube bank characteristics for this study are presented as follows: ST=0.04, SL=0.03, $\mathrm{Sd} = \sqrt{(\mathrm{ST}/2)^2 + \mathrm{SL}^2}$, and D=0.02 m.

The log-mean temperature difference is the appropriate form of ΔT to be used for this correlation analysis [3,31]. It is given as

$$\Delta\mathrm{T_{LMTD}} = \frac{\mathrm{T_i} - \mathrm{T_e}}{\mathrm{Ln}\left(\frac{\mathrm{T_w} - \mathrm{T_e}}{\mathrm{T_w} - \mathrm{T_i}}\right)} = \frac{\Delta\mathrm{T_e} - \Delta\mathrm{T_i}}{\mathrm{Ln}\left(\frac{\Delta\mathrm{T_e}}{\Delta\mathrm{T_i}}\right)} \tag{8}$$

After determining ΔT_{LMTD}, the heat transfer rate per unit length of the tubes can be calculated using the subsequent formula

$$\dot{\mathrm{Q}} = \mathrm{h\ S\ N_T \Delta T_{LMTD}} \tag{9}$$

where N_T is the total number of tubes.

The pressure drop ΔP is an important measure related to the determination of tube banks performances. This drop is the irreversible pressure loss between the entrance and the exit of the tube bank. This measure can be obtained using Eq. (10)

$$\Delta P = f \, X \, N_L \frac{\rho V_m^2}{2} \tag{10}$$

where $(\rho V^2/2)$ is the dynamic pressure. The friction factor ƒ and the correction factor X are computed in parallel forms [3,27,31].

A power directly related to the pressure drop is necessary to ensure the fluid displacement through a tube bank. It may be expressed as

$$\dot{w}_{pump} = \dot{V} \, \Delta P = \frac{\dot{m}}{\rho} \Delta P \tag{11}$$

2.2 Thermophysical Characteristics of Nanofluids

The thermophysical characteristics of nanofluids are indispensable to consider for optimizing their heat transfer performance. These properties are, respectively, the density, specific heat, thermal expansion, dynamic viscosity, and thermal conductivity. The addition of nanoparticles profoundly modifies these properties. Many parameters characterizing these nanoparticles (nature and size of the nanoparticles, volume fraction, conductivity of the base fluid, conductivity of the nanoparticles, temperature of the medium, etc.) can be evaluated. These parameters can considerably affect the thermophysical characteristics of the nanofluid obtained.

The effective thermophysical properties of the nanofluid will be approximated by different relationships drawn from the literature or those established in this work.

Using classical formulas derived for two-phase mixing, the nanofluid density can be calculated through various steps. The nanofluid density is given as a function of particle volume concentration and individual properties [31,32]

$$\rho_{nf} = \frac{m_f + m_s}{V_f + V_s} = \frac{m_f \rho_f + m_s \rho_s}{V_f + V_s} \tag{12}$$

A specific model can be used to determine the specific heat of a nanofluid. It is presented as

$$\left(C_p\right)_{nf} = (1-\varphi)\left(C_p\right)_f + \varphi\left(C_p\right)_n \tag{13}$$

The density can be computed from the model of Xuan and Roetzel [25], and Bianco *et al.,* [32]. It is given as

$$\left(\rho C_p\right)_{nf} = (1-\varphi)\left(\rho C_p\right)_f + \varphi\left(\rho C_p\right)_n \tag{14}$$

Maxwell's model and its derivatives are probably the most widely used in previous studies [33,34]. This basic model assumes that the fluid contains many spherical particles of the same diameter and disperses in a weak concert.

Maxwell's formula is given by

$$\frac{K_{nf}}{K_f} = \frac{K_s(1-2\beta_1)+2K_f+2\varphi[K_s(1-\beta_1)-K_f]}{K_s(1-2\beta_1)+2K_f+\varphi[K_s(1-\beta_1)-K_f]} \quad (15)$$

To calculate the value of the volume expansion coefficient (β) for nanofluids, many authors have followed the approach used in the first works that treated nanofluids. By analogy with the considered relationship, the following expression is deduced by Jehad and Hashim [35]

$$\beta = (1-\varphi)(\beta_f + \varphi\beta_s) \quad (16)$$

The dynamic viscosity can be calculated from the viscosity of the base fluid and the volume fraction of the nanofluid. For what follows, two models will be quoted for the calculation of the apparent viscosities. Brinkman developed Einstein's formula to cover a wide range of volume concentrations [35]

$$\mu_{nf} = \frac{\mu_f}{(1-\varphi)^{2.5}} \quad (17)$$

Although it is a technique still under development, the simulation of large turbulent structures is currently a practical tool for the engineer. It enables the simulation of configurations that are extremely similar to those found in the industrial sector. In this section, a numerical simulation will be performed for an aluminum structure with various nanofluids, including: copper, copper oxide, aluminum, aluminum oxide, and others.

The rheological behavior of nanofluids can be found through experimental studies in previous works and references. It allows us to highlight the effect of temperature and concentration on the progress of the characteristics of nanofluids. In this part, a complete study will be carried out on various nanofluids to examine the effect of concentration and temperature on their rheological behavior.

Figure 4 to Figure 9 represent the evolution of the characteristics of the chosen nanofluids according to the temperature and the concentration Φ.

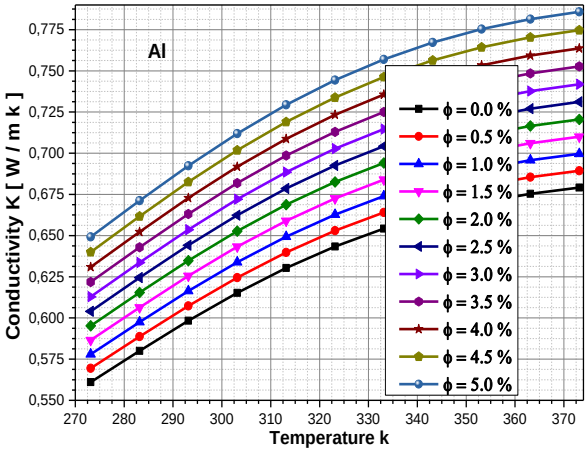

Fig. 4. Evolution of the conductivity as a function of temperature for Al at different concentrations

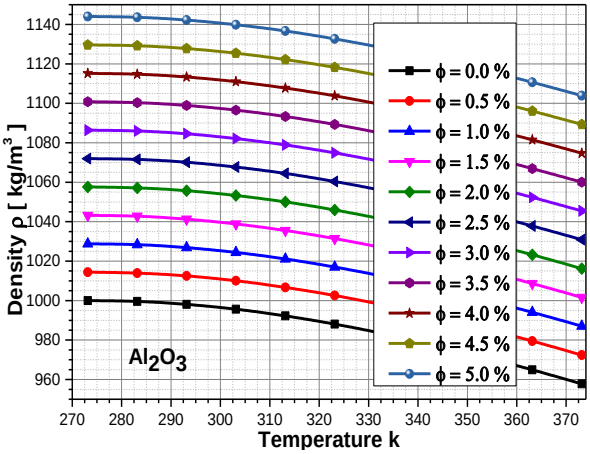

Fig. 5. Evolution of the density as a function of temperature for Al_2O_3 at different concentrations

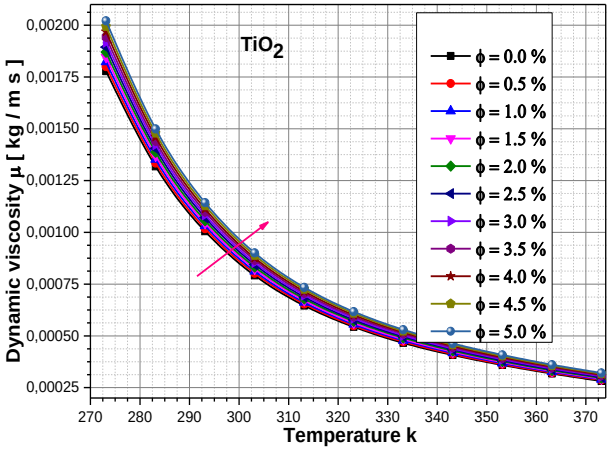

Fig. 6. Evolution of the dynamic viscosity as a function of temperature for TiO_2 at different concentrations

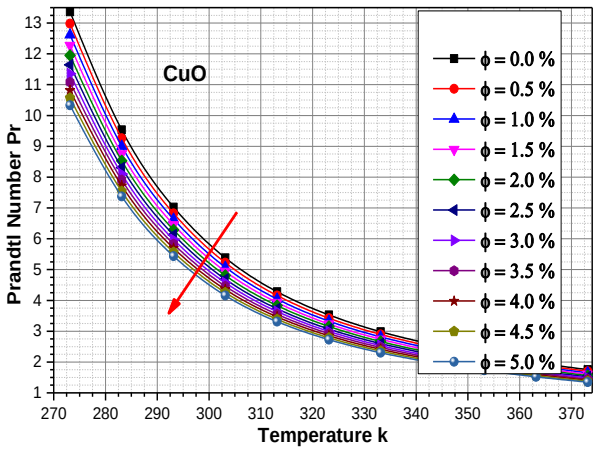

Fig. 7. Evolution of the Prandtl number as a function of temperature for CuO at different concentrations

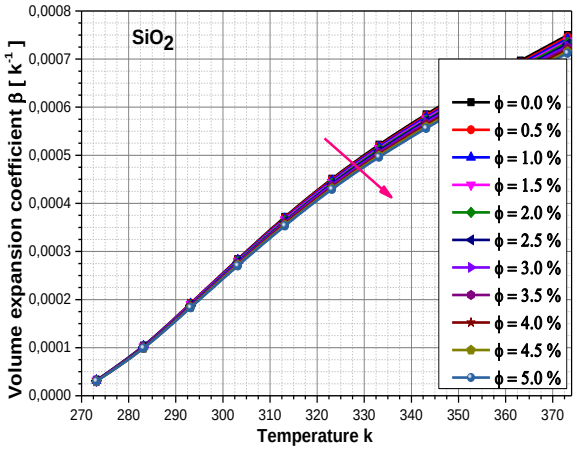

Fig. 8. Evolution of the volume expansion coefficient as a function of temperature for SiO_2 at different concentrations

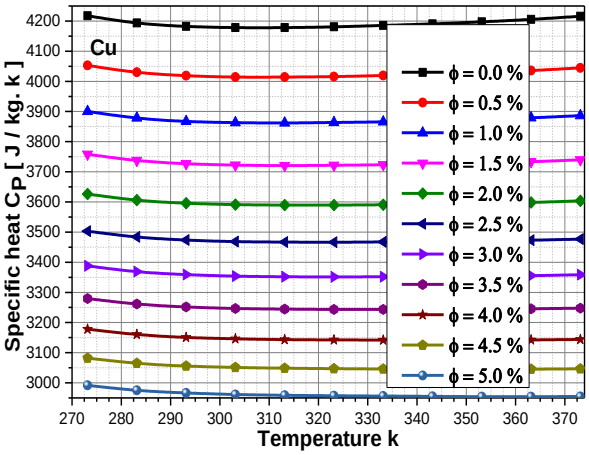

Fig. 9. Evolution of the specific heat as a function of temperature for Cu at different concentrations

The influence of the concentration Φ and the temperature variation is shown in the previous figures.

The augmentation of the temperature has an important effect on all parameters. The density, dynamic viscosity, Prandtl number and specific heat decrease with the temperature increasing. Contrarily, the conductivity and volume expansion increase with the temperature increasing. Table 1 gives some numerical values of various characteristics obtained for the concentration Φ range [0.5%-5%] and a fixed temperature of 293 K.

Table 1
Evolution of characteristics of various nanofluids according to the concentration Φ for T=293 K

Characteristics	Nanofluid	Base fluid	concentration Φ %									
			0,5	1	1,5	2	2,5	3	3,5	4	4,5	5
Conductivity ($W\ m^{-1}\ K^{-1}$)	AL	0,6	0,606	0,614	0,625	0,632	0,641	0,651	0,663	0,675	0,683	0,69
Density ($Kg\ m^{-3}$)	Al_2O_3	1000	1012	1025	1040	1055	1070	1085	1100	1115	1125	1143
Dynamic viscosity 10^{-3}($Kg\ m^{-1}\ s^{-1}$)	TiO_2	100	101	103	104	105	106	107	108	110	111	112
Prandtl number	CuO	7	6,9	6,7	6,65	6,6	6,5	6,3	6,1	5,9	5,7	5,5
Specific heat ($J\ kg^{-1}\ K^{-1}$)	Cu	4200	4040	3865	3740	3600	3480	3350	3255	3150	3060	2970
Volume expansion 10^{-4} (K^{-1})	SiO_2	2	1,998	1,997	1,995	1,994	1,992	1,99	1,988	1,987	1,983	1,98

The effect of concentration on conductivity, density, and dynamic viscosity is proportional according to a fixed temperature. The Prandtl number, specific heat, and volume expansion decrease with an increase in concentration.

The present results demonstrate better adequacy compared with those issued in previous works [1,6,36-38]. This similar evolution of the behavior of all tested nanofluids verifies the validity and accuracy of the applied model.

The interpolation expressions of the coefficients attached to the nanofluid parameters are determined numerically with high accuracy. The results of the interpolation are calculated for each temperature-concentration combination. The polynomial interpolations found for each nanofluid parameter are presented as follows

$$K(T)=A_0+A_1\times T+A_2\times T^2 \tag{18}$$

$$\mu(T)=B_0+B_1\times T+B_2\times T^2+B_3\times T^3+B_4\times T^4 \tag{19}$$

$$\rho(T)=C_0+C_1\times T+C_2\times T^2+C_3\times T^3+C_4\times T^4+C_5\times T^5+C_6\times T^6 \tag{20}$$

$$C_P(T)=D_0+D_1\times T+D_2\times T^2+D_3\times T^3+D_4\times T^4+D_5\times T^5+D_6\times T^6 \tag{21}$$

$$Pr(T)=E_0+E_1\times T+E_2\times T^2+E_3\times T^3+E_4\times T^4+E_5\times T^5+E_6\times T^6 \tag{22}$$

$$\beta(T)=F_0+F_1\times T+F_2\times T^2+F_3\times T^3+F_4\times T^4+F_5\times T^5 \tag{23}$$

2.3 Application on Tube Bank

The two-dimensional computational geometry is initially created with a width of 180mm and a height of 40mm. The diameter of each tube is 20 mm. The configuration consists of an array of circular tubes placed in a staggered arrangement. The array consists of 7 rows of tubes while the upper and lower tubes are used to generate the effect of the preceding tube over the next.

Other details of the studied configuration are indicated in Figure 10.

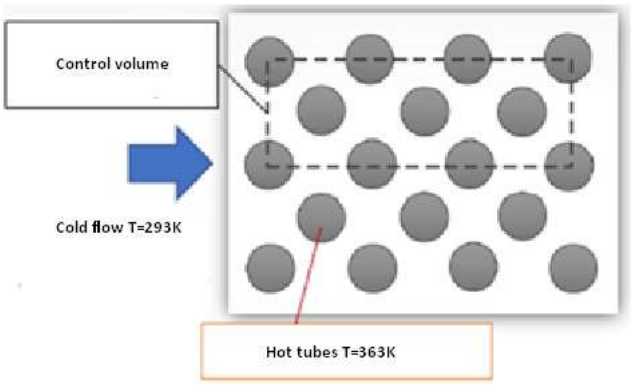

Fig. 10. Control volume of the study

The applied mass flow rate at the inlet boundary ranges from 0.01 kg/s to 3 Kg/s. The temperature of the tube wall is 363 K, and the temperature of the carrier fluid (H_2O) is 293 K.

All properties of nanofluids are introduced to the computational model through polynomial interpolations, as described in section 2.2. A hybrid mesh consisting of 90000 cells was created with to obtain more accurate results, especially near to the tube where a structured mesh was used to capture the boundary layer. Further details regarding the boundary conditions can be found in Figure 11.

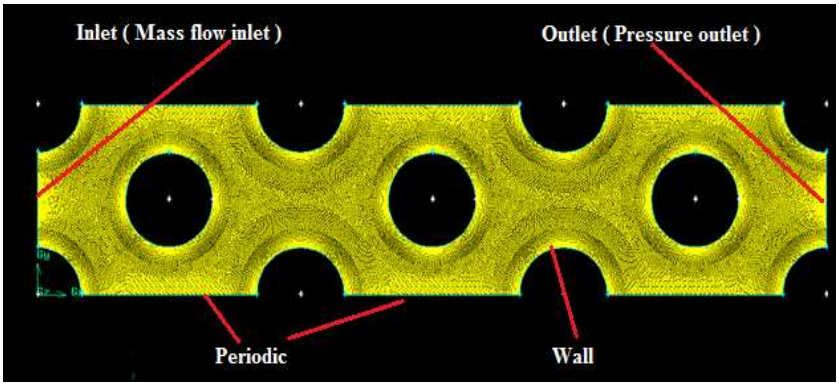

Fig. 11. Final mesh with defined boundary conditions

3. Results and Comments

Using a numerical approach that evolves presenting the means by which the governing equations of flow can be solved. The Ansys-Fluent software presents the problem description for the simulation in this step, essentially outlining the method it suggests for resolving the issues. The GAMBIT software is responsible for the conception of geometry, mesh generation, and inclusion of boundary conditions.

A visual criterion was employed to ensure that the computations would converge. It is based on the observation of the residual curves of the equation-derived conservation (these curves are given by FLUENT). Based on the history of iterations, it can be seen that the solution has converged when the residuals are low (less than 10E-3 in order). At this stage, the curves become stable, and the results are independent of the mesh.

Figure 12, Figure 13 and Figure 14 represent examples of the static pressure, temperature, and the velocity contours in the bundle of the exchanger for various nanofluids at different concentrations Φ.

Figure 12 shows that the contours vary as the concentration increases from 0.01 up to 5 %. Figure 12 also illustrates that the pressure at the entrance of a bundle of tubes for the nanofluids is higher than the outlet pressure. This variation explains the pressure drop at the outlet of the bundle.

In the pressure contour, a negative tendency behind the tube indicates that flow separation happens largely at the tube's uppermost point. A wake is formed behind the tube from that point forward. The high pressure at the tube's frontal section suggests a stagnation condition. It can be clearly seen in the figure that there is an early flow separation at a 45° longitudinal configuration. The heat transfer near the tube's surface region is greater than in other regions. This progression is logical because the surface of the tube is at a higher temperature due to the hot fluid moving inside the tube bank.

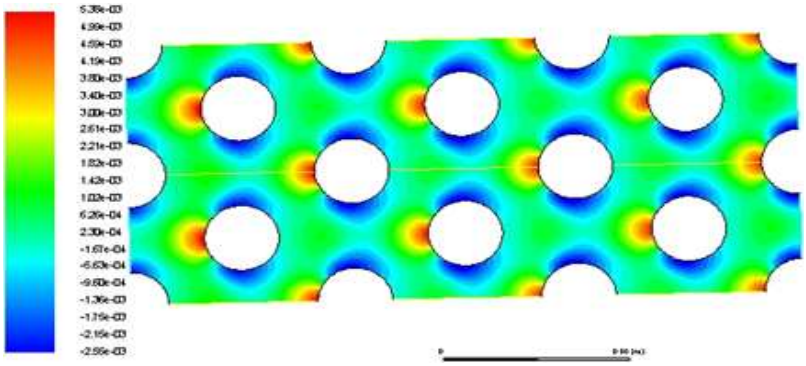

Fig. 12. Pressure contour in the bundles of the exchanger for CuO at Φ= 4% and m=0.5kg/s

The contours of the static temperature in the bundle of the exchanger are depicted in Figure 13. It can be shown that there is a transfer of heat through the tubes, especially on the walls of the tubes. So, there is a strong relationship between the temperature and the mass flow rate, which is reflected in the heat transfer rate. Also, the type of nanofluid used has severe effects on convection heat transfer.

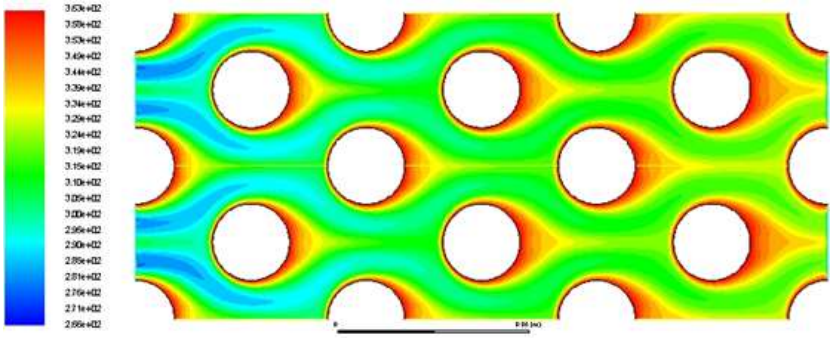

Fig. 13. Temperature contour in the bundles of the exchanger for SiO_2 at Φ=1% and m=0.05kg/s

Figure 14 depicts the contours of the velocity in the tube bank when the concentration has been changed from 0.01 to 5%. Cross flow over tubes produces intricate flow patterns. A boundary layer is generated when the fluid approaches the tube and surrounds it. This boundary layer encircles the tube. In the mid-plane, the fluid particles will collide with the tube at the stagnation point. At this point, the fluid particles bring the fluid to a complete stop and boost the pressure. While the fluid velocity increases, the pressure drops in the flow direction. At lower velocities, the carrier fluid entirely encircles the tube and follows the cylinder's form. Therefore, Figure 14 shows that the

velocity has maximum values in the flow path where there is no contact with the bench tubes. These values decrease more in the flow path that directly collides with the tubes. The velocity values decrease in this zone with an increase in pressure. The figure also shows the minimum velocity at the stopping point and at the point where there is direct contact between the tubes and the flow. It finally illustrates the basic values of velocity after the cylinders.

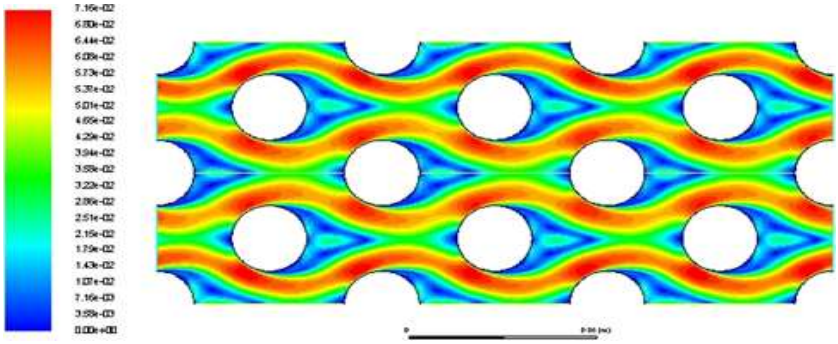

Fig. 14. Velocity contour in the bundles of the exchanger for Al at Φ=1% and m=1.0 kg/s

For higher velocities, the carrier fluid attaches the cylinder on the frontal side. It is too quick to stay connected to the surface as it approaches the cylinder's top. The separating point is known as the point where the boundary layer disconnects from the surface, leaving behind a wake. The wake region's flow is distinguished by random vortex generation and pressures substantially lower than the stagnation point pressure.

Figure 15 and Figure 16 represent the exit temperature and the maximum velocity according to the mass flow rate. These figures indicate that the increase in mass flow rate influences the maximum velocity and the exit temperature T_2. The exit temperature of Cu and CuO is found higher than that of other nanofluids. However, the obtained results are very satisfactory, the exit temperature can reach 358K and 326K for Al and Cu respectively at m=0.05 kg/s (the exit temperature T_2 of pure water equals 319K in this case). On the other hand, the process of cooling, where the temperature can be lowered to 338K, is better with Al. From these results, it was observed that the best nanofluid-concentration combination is given by CuO at Φ=3%.

On the other hand, the maximum velocity improves linearly with the mass flow rate. It can reach 0.0882 m/s and 0.0818 m/s for SiO_2 and Al_2O_3 at a mass flow rate of 3Kg/s and Φ=5%. These values correspond to Reynolds number equal to 1746 and 1758, respectively. The Reynolds number affects the velocity of the liquid heating which is better at slow velocities.

It can be noted that when the nanofluid moves rapidly in the bundle, the improvement of the heat exchange quality between the tubes and the fluid is good. The flow will be more turbulent in this situation. A difference of 13% in results was found compared with pure water.

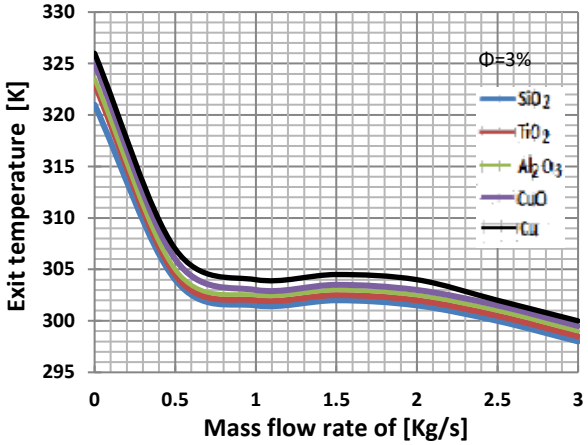

Fig. 15. Exit temperature as a function of mass flow rate

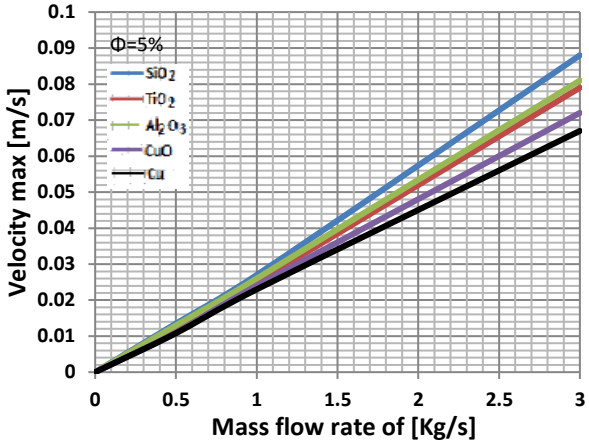

Fig. 16. Velocity max as a function of mass flow rate

Figure 17 and Figure 18 represent the variation of the Nusselt number and the heat transfer coefficient, respectively, with the mass flow rate for some nanofluids. The Nusselt numbers of SiO_2 and TiO_2 are greater than those of the other nanofluids (Al_2O_3, Al, Cu, CuO). They can reach up to 64% and 61% for SiO_2 and TiO_2, respectively, compared to water. On the other hand, the heat transfer coefficient is not always directly proportional to the Nusselt number. This happens when the thermal conductivity influences the heat transfer coefficient and the Nusselt number. A difference of 8 % in results was found compared with pure water for the Nusselt number.

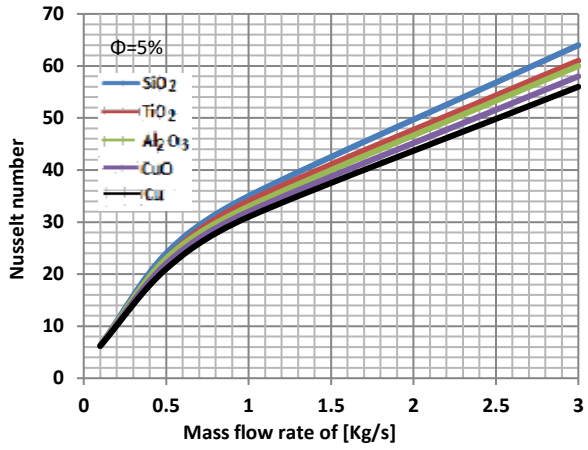

Fig. 17. Nusselt number as a function of mass flow rate

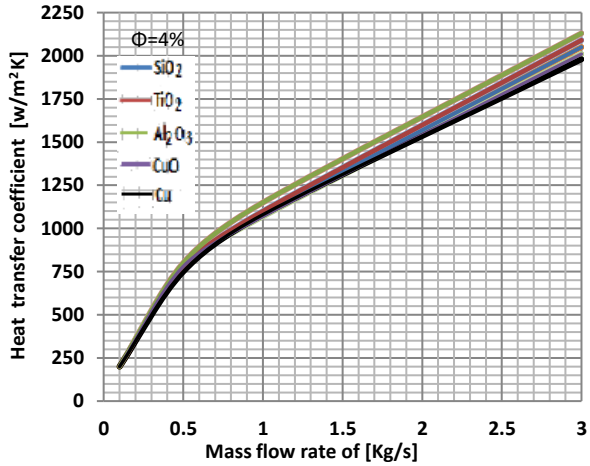

Fig. 18. Heat transfer coefficient as a function of mass flow rate

Figure 19 illustrates the effect of the mass flow rate on the heat rate for some nanofluids. This effect on both flow and heat transmission is significant. The heat rate is directly proportional to the convection heat coefficient h. The nanoparticles (Al_2O_3, TiO_2 and SiO_2) have the highest values, such as 62382 W, 61367 W and 60119 W, respectively. The concentration of nanoparticles considerably affects the increasing of the thermal conductivity. The best results are obtained using 3kg/s mass flow, yielding a Nusselt number of 64.

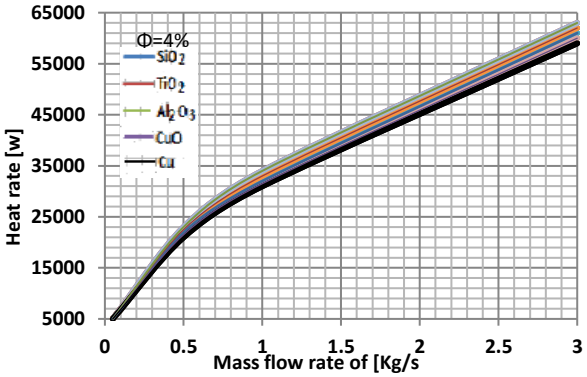

Fig. 19. Heat rate as a function of mass flow rate

One of the primary concerns in heat exchanger design is the estimation of pressure drop. Figure 20 shows the evolution of the pressure drop with the increase of the mass flow rate. The pressure drop is a representation of energy loss and is the most typical disadvantage of the staggered tube bank configuration. If the pressure drop in tube banks increases, the friction factor increases. This is lowering the total thermal performance of the system and increasing the pumping power. Consequently, this result influences the initial and operating costs of heat exchangers. The enhancement of the pressure drop is expected because of the turbulence in a flow field. As illustrated in Figure 20 and Figure 21, this could be owing to the smaller size of the wake generation in the case of tubes. The SiO_2 nanofluid has the greatest value and can reach up to 2514Pa, which requires 4.1 Joule of power to recover this pressure drop. The lower value computed is 1909 Pa for Cu, which needs 7.12 Joule compared to SiO_2.

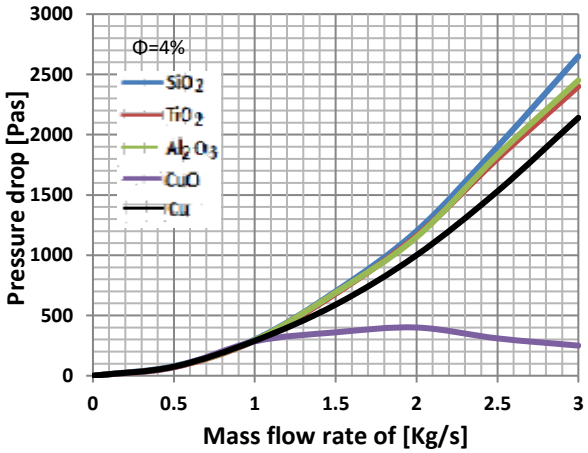

Fig. 20. Pressure drop as a function of mass flow rate

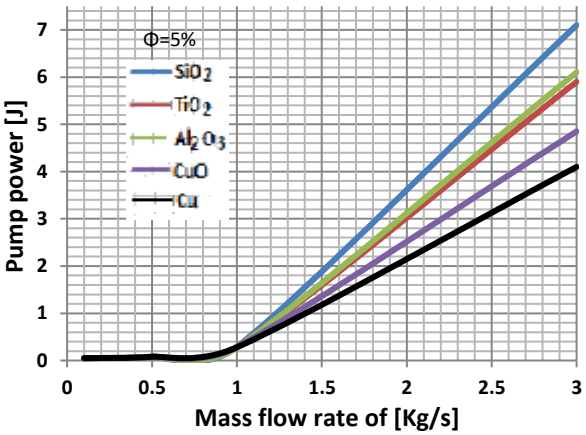

Fig. 21. Pump power as a function of mass flow rate

The results reveal that the enhancement of thermophysical properties of (SiO_2, Al_2O_3, TiO_2) is greater than that of metal nanoparticles (Al, Cu). Similar observations have been reported in previous studies. This similarity finding is for the enhancement of Nusselt number, pump power, pressure drop and heat transfer coefficient for (SiO_2, Al_2O_3, TiO_2) [36-38].

4. Conclusion

This work presents and investigates numerically the flow and heat transfer in a heat exchanger bundle. It is based on the exploitation of some common and available nanoparticles at different concentrations in water as the base fluid.

In conclusion, various points are opted, and results indicate that the conductivity of fluid can be improved by adding a nanoparticle. The addition of nanoparticles improves heat transfer. The choice of the nanoparticle plays a significant role in the enhancement of the heat transfer process and fluid flow characteristics.

The conducted simulations show that the heat flux and pressure drop increase with an increasing number of rows of tubes. However, the heat transfer ferocity becomes almost stable when the number of rows is more than five.

It was established that an enhancement in the concentration of nanoparticles negatively affects the velocity of the liquid. The nanofluid CuO/H_2O yields the best results in terms of velocity, temperature, Nusselt number, h and Q, especially at Φ=3%.

The pressure drop for CuO will be less valuable in comparison with other nanoparticles. The particle diameter of CuO is 23.6 nm and 38.5 nm for Al_2O_3. The diameter of the particle also affects the roughness and fouling of the carrier fluid. This influence negatively affects the heat exchanger performance with time, especially, on the outer surfaces of tubes.

The addition of nanoparticles augments the thermal conductivity of the base fluid. This allows the obtained nanofluid to absorb and dissipate heat more effectively. This can lead to better performance and potentially smaller heat exchanger sizes, which is advantageous in various industrial applications. However, it is necessary to consider the cost as well as the stability of nanofluids for useful implementation. It is also appropriate to prefer a geometry that provides a good thermal exchange and a minimum pressure drop for an adequate design.

The Nusselt numbers of SiO_2 and TiO_2 are greater than those of other nanofluids (Al_2O_3, Al, Cu, CuO). They can reach up to 64% and 61% for SiO_2 and TiO_2, respectively, compared to water. For a fixed temperature, the effect of the concentration on the conductivity, density, and dynamic viscosity, is proportional for all considered nanofluids. On the other hand, the Prandtl number, specific heat, and volume expansion decrease with an increase in concentration. The improvement in the exit temperature at m=0.05kg/s can reach up to 12.2% and 2.1% for Al and Cu, respectively, compared to water.

References

[1] Khan, W. A., J. R. Culham, and M. M. Yovanovich. "Convection heat transfer from tube banks in crossflow: Analytical approach." *International Journal of Heat and Mass Transfer* 49, no. 25-26 (2006): 4831-4838. https://doi.org/10.1016/j.ijheatmasstransfer.2006.05.042

[2] Lee, HoSung. *Thermal design: heat sinks, thermoelectrics, heat pipes, compact heat exchangers, and solar cells*. John Wiley & Sons, 2010. https://doi.org/10.1002/9780470949979

[3] Incropera, Frank P., and David P. Dewitt. *Fundamental of heat and mass transfer*. John Wiley and Sons, 2007.

[4] Ahmed, M. Salem, Mohamed R. Abdel Hady, and G. Abdallah. "Experimental investigation on the performance of chilled-water air conditioning unit using alumina nanofluids." *Thermal Science and Engineering Progress* 5 (2018): 589-596. https://doi.org/10.1016/j.tsep.2017.07.002

[5] Sreedevi, P., P. Sudarsana Reddy, and Ali Chamkha. "Heat and mass transfer analysis of unsteady hybrid nanofluid flow over a stretching sheet with thermal radiation." *SN Applied Sciences* 2, no. 7 (2020): 1222. https://doi.org/10.1007/s42452-020-3011-x

[6] Yu, Wei, and Huaqing Xie. "A review on nanofluids: preparation, stability mechanisms, and applications." *Journal of Nanomaterials* 2012, no. 1 (2012): 435873. https://doi.org/10.1155/2012/435873

[7] Dey, Debashis, Pankaj Kumar, and Sikata Samantaray. "A review of nanofluid preparation, stability, and thermo-physical properties." *Heat Transfer-Asian Research* 46, no. 8 (2017): 1413-1442. https://doi.org/10.1002/htj.21282

[8] Özerinç, Sezer, Sadık Kakaç, and Almıla Güvenç Yazıcıoğlu. "Enhanced thermal conductivity of nanofluids: a state-of-the-art review." *Microfluidics and Nanofluidics* 8 (2010): 145-170. https://doi.org/10.1007/s10404-009-0524-4
[9] Sonawane, Sandipkumar, Kaustubh Patankar, Ankit Fogla, Bhalchandra Puranik, Upendra Bhandarkar, and S. Sunil Kumar. "An experimental investigation of thermo-physical properties and heat transfer performance of Al_2O_3-Aviation Turbine Fuel nanofluids." *Applied Thermal Engineering* 31, no. 14-15 (2011): 2841-2849. https://doi.org/10.1016/j.applthermaleng.2011.05.009
[10] Shahrul, I. M., I. M. Mahbubul, S. S. Khaleduzzaman, R. Saidur, and M. F. M. Sabri. "A comparative review on the specific heat of nanofluids for energy perspective." *Renewable and Sustainable Energy Reviews* 38 (2014): 88-98. https://doi.org/10.1016/j.rser.2014.05.081
[11] Chandrasekar, M., S. Suresh, and T. Senthilkumar. "Mechanisms proposed through experimental investigations on thermophysical properties and forced convective heat transfer characteristics of various nanofluids-A review." *Renewable and Sustainable Energy Reviews* 16, no. 6 (2012): 3917-3938. https://doi.org/10.1016/j.rser.2012.03.013
[12] Bozorgan, Navid, and Maryam Shafahi. "Performance evaluation of nanofluids in solar energy: a review of the recent literature." *Micro and Nano Systems Letters* 3 (2015): 1-15. https://doi.org/10.1186/s40486-015-0014-2
[13] Buongiorno, Jacopo, Lin-Wen Hu, Sung Joong Kim, Ryan Hannink, B. A. O. Truong, and Eric Forrest. "Nanofluids for enhanced economics and safety of nuclear reactors: an evaluation of the potential features, issues, and research gaps." *Nuclear Technology* 162, no. 1 (2008): 80-91. https://doi.org/10.13182/NT08-A3934
[14] Usri, N. A., W. H. Azmi, R. Mamat, and K. Abdul Hamid. "Forced convection heat transfer using water-ethylene glycol (60: 40) based nanofluids in automotive cooling system." *International Journal of Automotive and Mechanical Engineering* 11, no. 1 (2015): 2747-2755. https://doi.org/10.15282/ijame.11.2015.508.0231
[15] Handoyo, Ekadewi Anggraini, Christian Ivan Soeyanto, and Sutrisno Sutrisno. "Experimental Study on Effect of Nano ZnO on the Cooling Performance of Motorcycle Radiator." *Journal of Advanced Research in Fluid Mechanics and Thermal Sciences* 100, no. 2 (2022): 169-180. https://doi.org/10.37934/arfmts.100.2.169180
[16] Sudarmadji, Sudarmadji, Sugeng Hadi Susilo, and Asrori Asrori. "The Combined Method to Improve Heat Transfer Coefficient on Heat Exchanger." In *Heat Transfer-Fundamentals, Enhancement and Applications*. IntechOpen, 2022. https://doi.org/10.5772/intechopen.105880
[17] Pandya, Naimish S., Harshang Shah, Maysam Molana, and Arun Kumar Tiwari. "Heat transfer enhancement with nanofluids in plate heat exchangers: A comprehensive review." *European Journal of Mechanics-B/Fluids* 81 (2020): 173-190. https://doi.org/10.1016/j.euromechflu.2020.02.004
[18] Sarafraz, M. M., and F. J. E. T. Hormozi. "Heat transfer, pressure drop and fouling studies of multi-walled carbon nanotube nano-fluids inside a plate heat exchanger." *Experimental Thermal and Fluid Science* 72 (2016): 1-11. https://doi.org/10.1016/j.expthermflusci.2015.11.004
[19] Shahrul, I. M., I. M. Mahbubul, R. Saidur, S. S. Khaleduzzaman, and M. F. M. Sabri. "Performance evaluation of a shell and tube heat exchanger operated with oxide based nanofluids." *Heat and Mass Transfer* 52 (2016): 1425-1433. https://doi.org/10.1007/s00231-015-1664-6
[20] Wang, Yongqing, Xin Gu, Zunlong Jin, and Ke Wang. "Characteristics of heat transfer for tube banks in crossflow and its relation with that in shell-and-tube heat exchangers." *International Journal of Heat and Mass Transfer* 93 (2016): 584-594. https://doi.org/10.1016/j.ijheatmasstransfer.2015.10.018
[21] Chon, Chan Hee, Kenneth D. Kihm, Shin Pyo Lee, and Stephen US Choi. "Empirical correlation finding the role of temperature and particle size for nanofluid (Al_2O_3) thermal conductivity enhancement." *Applied Physics Letters* 87, no. 15 (2005). https://doi.org/10.1063/1.2093936
[22] Xue, Q., and Wen-Mei Xu. "A model of thermal conductivity of nanofluids with interfacial shells." *Materials Chemistry and Physics* 90, no. 2-3 (2005): 298-301. https://doi.org/10.1016/j.matchemphys.2004.05.029
[23] Paul, G., M. Chopkar, I. Manna, and P. K. Das. "Techniques for measuring the thermal conductivity of nanofluids: a review." *Renewable and Sustainable Energy Reviews* 14, no. 7 (2010): 1913-1924. https://doi.org/10.1016/j.rser.2010.03.017
[24] Wei, Xiaohao, and Liqiu Wang. "Synthesis and thermal conductivity of microfluidic copper nanofluids." *Particuology* 8, no. 3 (2010): 262-271. https://doi.org/10.1016/j.partic.2010.03.001
[25] Xuan, Yimin, and Wilfried Roetzel. "Conceptions for heat transfer correlation of nanofluids." *International Journal of Heat and Mass Transfer* 43, no. 19 (2000): 3701-3707. https://doi.org/10.1016/S0017-9310(99)00369-5
[26] Yu, Wenhua, David M. France, Jules L. Routbort, and Stephen U. S. Choi. "Review and comparison of nanofluid thermal conductivity and heat transfer enhancements." *Heat Transfer Engineering* 29, no. 5 (2008): 432-460. https://doi.org/10.1080/01457630701850851
[27] Corcione, Massimo. "Empirical correlating equations for predicting the effective thermal conductivity and dynamic viscosity of nanofluids." *Energy Conversion and Management* 52, no. 1 (2011): 789-793. https://doi.org/10.1016/j.enconman.2010.06.072

[28] Masoumi, N., N. Sohrabi, and A. Behzadmehr. "A new model for calculating the effective viscosity of nanofluids." *Journal of Physics D: Applied Physics* 42, no. 5 (2009): 055501. https://doi.org/10.1088/0022-3727/42/5/055501
[29] Murshed, S. M. Sohel, Say-Hwa Tan, and Nam-Trung Nguyen. "Temperature dependence of interfacial properties and viscosity of nanofluids for droplet-based microfluidics." *Journal of Physics D: Applied Physics* 41, no. 8 (2008): 085502. https://doi.org/10.1088/0022-3727/41/8/085502
[30] Shin, Donghyun, and Debjyoti Banerjee. "Specific heat of nanofluids synthesized by dispersing alumina nanoparticles in alkali salt eutectic." *International Journal of Heat and Mass Transfer* 74 (2014): 210-214. https://doi.org/10.1016/j.ijheatmasstransfer.2014.02.066
[31] Lienhard IV, John H., and John H. Lienhard V. *A Heat Transfer Textbook*. Dover Publications, 2020.
[32] Bianco, Vincenzo, Oronzio Manca, and Sergio Nardini. "Numerical simulation of water/Al_2O_3 nanofluid turbulent convection." *Advances in Mechanical Engineering* 2 (2010): 976254. https://doi.org/10.1155/2010/976254
[33] Yu, W., and and S. U. S. Choi. "The role of interfacial layers in the enhanced thermal conductivity of nanofluids: a renovated Maxwell model." *Journal of Nanoparticle Research* 5 (2003): 167-171. https://doi.org/10.1023/A:1024438603801
[34] Zhou, Shuang-Shuang, Muhammad Bilal, Muhammad Altaf Khan, and Taseer Muhammad. "Numerical analysis of thermal radiative maxwell nanofluid flow over-stretching porous rotating disk." *Micromachines* 12, no. 5 (2021): 540. https://doi.org/10.3390/mi12050540
[35] Jehad, D. G., and G. A. Hashim. "Numerical prediction of forced convective heat transfer and friction factor of turbulent nanofluid flow through straight channels." *Journal of Advanced Research in Fluid Mechanics and Thermal Sciences* 8, no. 1 (2015): 1-10.
[36] Hussein, Diyar F., and Yaser Alaiwi. "Efficiency Improvement of Double Pipe Heat Exchanger by using TiO_2/water Nanofluid." *CFD Letters* 16, no. 1 (2024): 43-54. https://doi.org/10.37934/cfdl.16.1.4354
[37] Kamel, Mohammed Saad, and Sherwan Mohammed Najm. "Heat transfer and fluid flow over a bank of circular tubes heat exchanger using nanofluids: CFD simulation." In *IOP Conference Series: Materials Science and Engineering*, vol. 928, no. 2, p. 022017. IOP Publishing, 2020. https://doi.org/10.1088/1757-899X/928/2/022017
[38] Ehsan, M. Monjurul, Shafi Noor, Sayedus Salehin, and AKM Sadrul Islam. "Application of nanofluid in heat exchangers for energy savings." In *Thermofluid Modeling for Energy Efficiency Applications*, pp. 73-101. Academic Press, 2016. https://doi.org/10.1016/B978-0-12-802397-6.00004-X